SEMIDISCRETE AND DISCRETE WELL-POSEDNESS OF SHOCK FILTERING

Martin Welk,[1] and Joachim Weickert[1]

[1] *Mathematical Image Analysis Group*
Faculty of Mathematics and Computer Science, Bldg. 27
Saarland University, 66041 Saarbruecken, Germany
{welk,weickert}@mia.uni-saarland.de

Abstract While shock filters are popular morphological image enhancement methods, no well-posedness theory is available for their corresponding partial differential equations (PDEs). By analysing the dynamical system of ordinary differential equations that results from a space discretisation of a PDE for 1-D shock filtering, we derive an analytical solution and prove well-posedness. Finally we show that the results carry over to the fully discrete case when an explicit time discretisation is applied.

Keywords: Shock filters, analytical solution, well-posedness, dynamical systems.

1. Introduction

Shock filters are morphological image enhancement methods where dilation is performed around maxima and erosion around minima. Iterating this process leads to a segmentation with piecewise constant segments that are separated by discontinuities, so-called shocks. This makes shock filtering attractive for a number of applications where edge sharpening and a piecewise constant segmentation is desired.

In 1975 the first shock filters have been formulated by Kramer and Bruckner in a fully discrete manner [6], while first continuous formulations by means of partial differential equations (PDEs) have been developed in 1990 by Osher and Rudin [8]. The relation of these methods to the discrete Kramer–Bruckner filter became clear several years later [4, 12]. PDE-based shock filters have been investigated in a number of papers. Many of them proposed modifications with higher robustness under noise [1, 3, 5, 7, 12], but also coherence-enhancing shock filters [14] and numerical schemes have been studied [11].

Let us consider some continuous d-dimensional initial image $f : \mathbb{R}^d \to \mathbb{R}$. In the simplest case of a PDE-based shock filter [8], one obtains a filtered

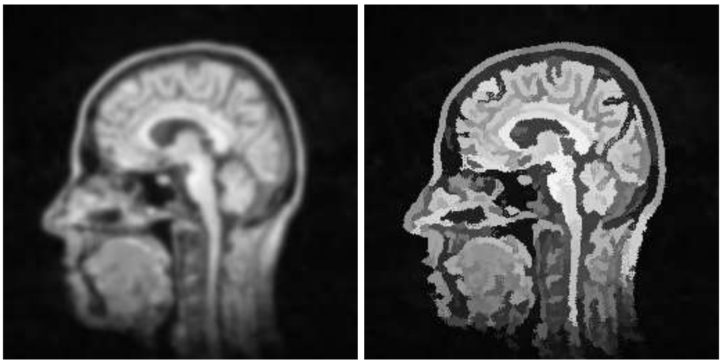

Figure 1. LEFT: Original image. RIGHT: After applying the Osher–Rudin shock filter.

version $u(x,t)$ of $f(x)$ by solving the evolution equation

$$\partial_t u = -\mathrm{sgn}(\Delta u)\,|\nabla u| \qquad (t \geq 0)$$

with f as initial condition, i. e. $u(0,x) = f(x)$. Experimentally one observes that within finite "evolution time" t, a piecewise constant, segmentation-like result is obtained (see Fig. 1).

Specialising to the one-dimensional case, we obtain

$$\partial_t u = -\mathrm{sgn}(\partial_{xx} u)\,|\partial_x u| = \begin{cases} |\partial_x u|, & \partial_{xx} u < 0, \\ -\,|\partial_x u|, & \partial_{xx} u > 0, \\ 0, & \partial_{xx} u = 0. \end{cases} \qquad (1)$$

It is clearly visible that this filter performs dilation $\partial_t u = |\partial_x u|$ in concave segments of u, while in convex parts the erosion process $\partial_t u = -|\partial_x u|$ takes place. The time t specifies the radius of the interval (a 1-D disk) $[-t, t]$ as structuring element. For a derivation of these PDE formulations for classical morphological operations, see e.g. [2].

While there is clear experimental evidence that shock filtering is a useful operation, no analytical solutions and well-posedness results are available for PDE-based shock filters. In general this problem is considered to be too difficult, since shock filters have some connections to classical ill-posed problems such as backward diffusion [8, 7].

The goal of the present paper is to we show that it is possible to establish analytical solutions and well-posedness as soon as we study the *semidiscrete* case with a spatial discretisation and a continuous time parameter t. This case is of great practical relevance, since digital images already induce a natural space discretisation. For the sake of simplicity we restrict ourselves to the 1-D case. We also show that these results carry over to the fully discrete case with an explicit (Euler forward) time discretisation.

Our paper is organised as follows: In Section 2 we present an analytical solution and a well-posedness proof for the semidiscrete case, whereas corresponding fully discrete results are given in Section 3. Conclusions are presented in Section 4.

2. The Semidiscrete Model

Throughout this paper, we are concerned with a spatial discretisation of (1) which we will describe now.

PROBLEM. *Let* $(\ldots, u_0(t), u_1(t), u_2(t), \ldots)$ *be a time-dependent real-valued signal which evolves according to*

$$\dot{u}_i = \begin{cases} \max(u_{i+1} - u_i, u_{i-1} - u_i, 0), & 2u_i > u_{i+1} + u_{i-1}, \\ \min(u_{i+1} - u_i, u_{i-1} - u_i, 0), & 2u_i < u_{i+1} + u_{i-1}, \\ 0, & 2u_i = u_{i+1} + u_{i-1} \end{cases} \qquad (2)$$

with the initial conditions

$$u_i(0) = f_i. \qquad (3)$$

Assume further that the signal is either of infinite length or finite with reflecting boundary conditions.

Like (1), this filter switches between dilation and erosion depending on the local convexity or concavity of the signal. Dilation and erosion themselves are modeled by upwind-type discretisations [9], and $\dot{u}_i$ denotes the time derivative of $u_i(t)$.

It should be noted that in case $2u_i > u_{i+1} + u_{i-1}$ the two neighbour differences $u_{i+1} - u_i$ and $u_{i-1} - u_i$ cannot be simultaneously positive; with the opposite inequality they can't be simultaneously negative. In fact, always when the maximum or minimum in (2) does not select its third argument, zero, it returns the absolutely smaller of the neighbour differences.

No modification of (2) is needed for finite-length signals with reflecting boundary conditions. In this case, each boundary pixel has one vanishing neighbour difference.

In order to study the solution behaviour of this system, we have to specify the possible solutions, taking into account that the right-hand side of (2) may involve discontinuities. We say that a time-dependent signal $u(t) = (\ldots, u_1(t), u_2(t), u_3(t) \ldots)$ is a *solution* of (2) if

(I) each u_i is a piecewise differentiable function of t,

(II) each u_i satisfies (2) for all times t for which $\dot{u}_i(t)$ exists,

(III) for $t = 0$, the right-sided derivative $\dot{u}_i^+(0)$ equals the right-hand side of (2) if $2u_i(0) \neq u_{i+1}(0) + u_{i-1}(0)$.

We state now our main result.

THEOREM 1 (WELL-POSEDNESS) *For our Problem, assume that the equality $f_{k+1} - 2f_k + f_{k-1} = 0$ does not hold for any pixel f_k which is not a local maximum or minimum of f. Then the following are true:*

(i) ***Existence and uniqueness:*** *The Problem has a unique solution for all $t \geq 0$.*

(ii) ***Maximum–minimum principle:*** *If there are real bounds a, b such that $a < f_k < b$ holds for all k, then $a < u_k(t) < b$ holds for all k and all $t \geq 0$.*

(iii) l_∞***-stability:*** *There exists a $\delta > 0$ such that for any initial signal $\tilde{f}$ with $\|\tilde{f} - f\|_\infty < \delta$ the corresponding solution $\tilde{u}$ satisfies the estimate*

$$\|\tilde{u}(t) - u(t)\|_\infty < \|\tilde{f} - f\|_\infty$$

for all $t > 0$. The solution therefore depends l_∞-continuously on the initial conditions within a neighbourhood of f.

(iv) ***Total variation preservation:*** *If the total variation of f is finite, then the total variation of u at any time $t \geq 0$ equals that of f.*

(v) ***Steady state:*** *For $t \to \infty$, the signal u converges to a piecewise constant signal. The jumps in this signal are located at the steepest slope positions of the original signal.*

All statements of this theorem follow from an explicit analytical solution of the Problem that will be described in the following proposition.

PROPOSITION 2 (ANALYTICAL SOLUTION) *For our standard problem, let the segment $(f_1, \ldots, f_m)$ be strictly decreasing and concave in all pixels. Assume that the leading pixel f_1 is either a local maximum or a neighbour to a convex pixel $f_0 > f_1$. Then the following hold for all $t \geq 0$:*

(i) If f_1 is a local maximum of f, $u_1(t)$ is a local maximum of $u(t)$.

(ii) If f_1 is neighbour to a convex pixel $f_0 > f_1$, then $u_1(t)$ also has a convex neighbour pixel $u_0(t) > u_1(t)$.

(iii) The segment $(u_1, \ldots, u_m)$ remains strictly decreasing and concave in all pixels. The grey values of all pixels at time t are given by

$$\begin{aligned} u_k(t) = C \cdot \left(1 + (-1)^k \mathrm{e}^{-2t} - \mathrm{e}^{-t} \sum_{j=0}^{k-2} \frac{t^j}{j!}(1 + (-1)^{k-j})\right) \\ + \mathrm{e}^{-t} \sum_{j=0}^{k-2} \frac{t^j}{j!} f_{k-j} - (-1)^k f_1 \mathrm{e}^{-t} \left(\mathrm{e}^{-t} - \sum_{j=0}^{k-2} \frac{(-t)^j}{j!}\right) \end{aligned} \tag{4}$$

for $k = 1, \ldots, m$, where $C = f_1(0)$ if f_1 is a local maximum of f, and $C = \frac{1}{2}(f_0(0) + f_1(0))$ otherwise.

(iv) At no time $t \geq 0$, the equation $2u_i(t) = u_{i+1}(t) + u_{i-1}(t)$ becomes true for any $i \in \{1, \ldots, m\}$.

Analogous statements hold for increasing concave and for convex signal segments.

In a signal that contains no locally flat pixels (such with $2f_i = f_{i+1} + f_{i-1}$), each pixel belongs to a chain of either concave or convex pixels led by an extremal pixel or an "inflection pair" of a convex and a concave pixel. Therefore Proposition 2 completely describes the dynamics of such a signal. Let us prove this proposition.

PROOF. We show in steps (i)–(iii) that the claimed evolution equations hold as long as the initial monotonicity and convexity properties of the signal segment prevail. Step (iv) then completes the proof by demonstrating that the evolution equations preserve exactly these monotonicity and convexity requirements.

(i) From (2) it is clear that any pixel u_i which is extremal at time t has $\dot{u}_i(t) = 0$ and therefore does not move. Particularly, if f_1 is a local maximum of f, then $u_1(t)$ remains constant as long as it continues to be a maximum.

(ii) If $u_0 > u_1$, u_0 is convex and u_1 concave for $t \in [0, T)$. Then we have for these pixels

$$\begin{aligned} \dot{u}_0 &= u_1 - u_0 \ , \\ \dot{u}_1 &= u_0 - u_1 \end{aligned} \tag{5}$$

which by the substitutions $y := \frac{1}{2}(u_0 + u_1)$ and $v := u_1 - u_0$ becomes

$$\begin{aligned} \dot{y} &= 0 \ , \\ \dot{v} &= -2v \ . \end{aligned}$$

This system of linear ordinary differential equations (ODEs) has the solution $y(t) = y(0) = C$ and $v(t) = v(0) \exp(-2t)$. Backsubstitution gives

$$\begin{aligned} u_0(t) &= C \cdot (1 - \mathrm{e}^{-2t}) + f_0 \mathrm{e}^{-2t} \ , \\ u_1(t) &= C \cdot (1 - \mathrm{e}^{-2t}) + f_1 \mathrm{e}^{-2t} \ . \end{aligned} \tag{6}$$

This explicit solution is valid as long as the convexity and monotonicity properties of u_0 and u_1 do not change.

(iii) Assume the monotonicity and convexity conditions required by the proposition for the initial signal hold for $u(t)$ for all $t \in [0, T)$. Then we have in all cases, defining C as in the proposition, the system of ODEs

$$\begin{aligned} \dot{u}_1 &= -2(u_1 - C) \ , \\ \dot{u}_k &= u_{k-1} - u_k \ , \qquad k = 2, \ldots, m \end{aligned} \tag{7}$$

for $t \in [0,T)$. We substitute further $v_k := u_k - C$ for $k = 1,\ldots,m$ as well as $w_1 := v_1$ and $w_k := v_k + (-1)^k v_1$ for $k = 2,\ldots,m$. This leads to the system

$$\begin{aligned} \dot{w}_1 &= -2w_1\ , \\ \dot{w}_2 &= -w_2\ , \\ \dot{w}_k &= w_{k-1} - w_k\ , \qquad k = 3,\ldots,m\ . \end{aligned} \tag{8}$$

This system of linear ODEs has the unique solution

$$\begin{aligned} w_1(t) &= w_1(0)\mathrm{e}^{-2t}\ , \\ w_k(t) &= \mathrm{e}^{-t}\sum_{j=0}^{k-2}\frac{t^j}{j!}w_{k-j}(0)\ , \qquad k = 2,\ldots,m \end{aligned}$$

which after reverse substitution yields (4) for all $t \in [0,T]$.

(iv) Note that (5) and (7) are systems of linear ODEs which have the unique explicit solutions (6) and (4) for all $t > 0$. As long as the initial monotonicity and convexity conditions are satisfied, the solutions of (2) coincide with those of the linear ODE systems.

We prove therefore that the solution (4) fulfils the monotonicity condition

$$u_k(t) - u_{k-1}(t) < 0\ , \qquad k = 2,\ldots,m$$

and the concavity conditions

$$u_{k+1}(t) - 2u_k(t) + u_{k-1}(t) < 0 \qquad k = 1,\ldots,m$$

for all $t > 0$ if they are valid for $t = 0$. To see this, we calculate first

$$\begin{aligned} u_k(t) - u_{k-1}(t) &= \mathrm{e}^{-t}\sum_{j=0}^{k-2}\frac{t^j}{j!}(f_{k-j} - f_{k-1-j}) \\ &\quad + 2\mathrm{e}^{-t}(-1)^{k-1}\left(\mathrm{e}^{-t} - \sum_{j=0}^{k-2}\frac{(-t)^j}{j!}\right)(f_1 - C)\ . \end{aligned}$$

By hypothesis, $f_{k-j} - f_{k-1-j}$ and $f_1 - C$ are negative. Further, $\exp(-t) - \sum_{j=0}^{k-2}(-t)^j/j!$ is the error of the (alternating) Taylor series of $\exp(-t)$, thus having the same sign $(-1)^{k-1}$ as the first neglected member. Consequently, the monotonicity is preserved by (4) for all $t > 0$.

Second, we have for $k = 2,\ldots,m-1$

$$\begin{aligned} u_{k+1}(t) - 2u_k(t) + u_{k-1}(t) &= \mathrm{e}^{-t}\sum_{j=0}^{k-1}\frac{t^j}{j!}(f_{k+1-j} - 2f_{k-j} + f_{k-j-1}) \\ &\quad + 4\mathrm{e}^{-t}(-t)^k\left(\sum_{j=0}^{k-1}\frac{(-t)^j}{j!}\right)(f_1 - C) \end{aligned}$$

which is seen to be negative by similar reasoning as above.

Concavity at $u_m(t)$ follows in nearly the same way. By extending (4) to $k = m + 1$, one obtains not necessarily the true evolution of u_{m+1} since that pixel is not assumed to be included in the concave segment. However, the true trajectory of u_{m+1} can only lie below or on that predicted by (4).

Third, if f_1 is a maximum of f, then $u_1(t)$ remains one for all $t > 0$ which also ensures concavity at u_1. If f_1 has a convex neighbour pixel $f_0 > f_1$, we have instead

$$u_2(t) - 2u_1(t) + u_0(t) = \mathrm{e}^{-t}(f_2 - 2f_1 + f_0) + 4\mathrm{e}^{-t}(1 - \mathrm{e}^{-t})(f_1 - C) < 0$$

which is again negative for all $t > 0$.

Finally, we remark that the solution (6) ensures $u_0(t) > u_1(t)$ for all $t > 0$ if it holds for $t = 0$. That convexity at u_0 is preserved can be established by analogous reasoning as for the concavity at u_1.

Since the solutions from the linear systems guarantee preservation of all monotonicity and convexity properties which initially hold for the considered segment, these solutions are the solutions of (2) for all $t > 0$. □

We remark that uniqueness fails if the initial signal contains non-extremal locally flat pixels. More details for this case are given in a preprint [15].

3. Explicit Time Discretisation

In the following we discuss an explicit time discretisation of our time-continuous system. We denote the time step by $\tau > 0$. The time discretisation of our Problem then reads as follows:

TIME-DISCRETE PROBLEM. *Let* $(\ldots, u_0^l, u_1^l, u_2^l, \ldots)$, $l = 0, 1, 2, \ldots$ *be a series of real-valued signals which satisfy the equations*

$$\frac{u_i^{l+1} - u_i^l}{\tau} = \begin{cases} \max(u_{i+1} - u_i, u_{i-1} - u_i, 0), & 2u_i > u_{i+1} + u_{i-1}, \\ \min(u_{i+1} - u_i, u_{i-1} - u_i, 0), & 2u_i < u_{i+1} + u_{i-1}, \\ 0, & 2u_i = u_{i+1} + u_{i-1} \end{cases} \tag{9}$$

with the initial conditions

$$u_i^0 = f_i \; ; \tag{10}$$

assume further that the signal is either of infinite length or finite with reflecting boundary conditions.

THEOREM 3 (TIME-DISCRETE WELL-POSEDNESS) *Assume that in the Time-Discrete Problem the equality* $f_{k+1} - 2f_k + f_{k-1} = 0$ *does not hold for any pixel* f_k *which is not a local maximum or minimum of* f*. Assume further that* $\tau < 1/2$*. Then the statements of Theorem 1 are valid for the solution* *of the Time-Discrete Problem if only $u_k(t)$ for $t > 0$ is replaced everywhere by u_k^l with $l = 0, 1, 2, \ldots$*

The existence and uniqueness of the solution of the Time-Discrete Problem for $l = 0, 1, 2, \ldots$ is obvious. Maximum–minimum principle, l_∞-stability, total variation preservation and the steady state property are immediate consequences of the following proposition. It states that for $\tau < 1/2$ all qualitative properties of the time-continuous solution transfer to the time-discrete case.

PROPOSITION 4 (TIME-DISCRETE SOLUTION) *Let u_i^l be the value of pixel i in time step l of the solution of our Time-Discrete Problem with time step size $\tau < 1/2$. Then the following hold for all $l = 0, 1, 2, \ldots$:*

(i) If u_1^l is a local maximum of u^l, then u_1^{l+1} is a local maximum of u^{l+1}.

(ii) If u_1^l is a concave pixel neighbouring to a convex pixel $u_0^l > u_1^l$, then u_1^{l+1} is again concave and has a convex neighbour pixel $u_0^{l+1} > u_1^{l+1}$.

(iii) If the segment $(u_1^l, \ldots, u_m^l)$ is strictly decreasing and concave in all pixels, and u_1^l is either a local maximum of u^l or neighbours to a convex pixel $u_0^l > u_1^l$, then the segment $(u_1^{l+1}, \ldots, u_m^{l+1})$ is strictly decreasing.

(iv) Under the same assumptions as in (iii), the segment $(u_1^{l+1}, \ldots, u_m^{l+1})$ is strictly concave in all pixels.

(v) If $2u_i^l = u_{i+1}^l + u_{i-1}^l$ holds for no pixel i, then $2u_i^{l+1} = u_{i+1}^{l+1} + u_{i-1}^{l+1}$ also holds for no pixel i.

(vi) Under the assumptions of (iii), all pixels in the range $i \in \{1, \ldots, m\}$ have the same limit $\lim_{l\to\infty} u_i^l = C$ with $C := u_1^l$ if u_1^l is a local maximum, or $C := \frac{1}{2}(u_0^l + u_1^l)$ if it neighbours to the convex pixel u_0^l.

Analogous statements hold for increasing concave and for convex signal segments.

PROOF. Assume first that u_1^l is a local maximum of u^l. >From the evolution equation (9) it is clear that $u_j^{l+1} \leq u_j^l + \tau(u_1^l - u_j^l)$ for $j = 0, 2$. For $\tau < 1$ this entails $u_j^{l+1} < u_1^l = u_1^{l+1}$, thus (i).

If instead u_i^l is a concave neighbour of a convex pixel $u_0^l > u_1^l$, then we have $u_1^{l+1} = u_1^l + \tau(u_0^l - u_1^l)$ and $u_0^{l+1} = u_0^l + \tau(u_1^l - u_0^l)$. Obviously, $u_0^{l+1} > u_1^{l+1}$ holds if and only if $\tau < 1/2$. For concavity, note that $u_2^{l+1} \leq u_2^l + \tau(u_1^l - u_2^l)$ and therefore $u_0^{l+1} - 2u_1^{l+1} + u_2^{l+1} \leq (1-\tau)(u_0^l - 2u_1^l + u_2^l) + 2\tau(u_1^l - u_0^l)$. The right-hand side is certainly negative for $\tau \leq 1/2$. An analogous argument secures convexity at pixel 0 which completes the proof of (ii).

In both cases we have $u_1^{l+1} \geq u_1^l$. Under the assumptions of (iii), (iv) we then have $u_k^{l+1} = u_k^l + \tau(u_{k-1}^l - u_k^l)$ for $k = 2, \ldots, m$. If $\tau < 1$, it follows that $u_k^l < u_k^{l+1} \leq u_{k-1}^l$ for $k = 2, \ldots, m$ which together with $u_1^{l+1} \geq u_1^l$ implies that $u_{k-1}^{l+1} > u_k^l$ for $k = 2, \ldots, m$ and therefore (iii).

For the concavity condition we compute

$$u_{k-1}^{l+1} - 2u_k^{l+1} + u_{k+1}^{l+1} = (1-\tau)(u_{k-1}^l - 2u_k^l + u_{k+1}^l) + \tau(u_{k-2}^l - 2u_{k-1}^l + u_k^l)$$

for $k = 3, \ldots, m-1$. The right-hand side is certainly negative for $\tau \leq 1$ which secures concavity in the pixels $k = 3, \ldots, m-1$. Concavity in pixel m for $\tau \leq 1$ follows from essentially the same argument; however, the equation is now replaced by an inequality since for pixel $m+1$ we know only that $u_{m+1}^{l+1} \leq u_{m+1}^l + \tau(u_m^l - u_{m+1}^l)$. If u_1^l is a local maximum and therefore $u_1^{l+1} = u_1^l$, we find for pixel 2 that $u_1^{l+1} - 2u_2^{l+1} + u_3^{l+1} = (1-\tau)(u_1^l - 2u_2^l + u_3^l) + \tau(u_2^l - u_1^l)$ which again secures concavity for $\tau \leq 1$. As was proven above, concavity in pixel 1 is preserved for $\tau \leq 1/2$ such that (iv) is proven.

Under the hypothesis of (v), the evolution of all pixels in the signal is described by statements (i)–(iv) or their obvious analoga for increasing and convex segments. The claim of (v) then is obvious.

Finally, addition of the equalities $C - u_1^{l+1} = (1-2\tau)(C - u_1^l)$ and $u_{i-1}^{l+1} - u_i^{l+1} = (1-\tau)(u_{i-1}^l - u_i^l)$ for $i = 2, \ldots, m$ implies that

$$C - u_k^{l+1} = (1-\tau)(C - u_k^l) - \tau(C - u_1^l) < (1-\tau)(C - u_k^l)$$

for all $k = 1, \ldots, m$. By induction, we have

$$C - u_k^{l+l'} \leq (1-\tau)^{l'}(C - u_k^l)$$

where the right-hand side tends to zero for $l' \to \infty$. Together with the monotonicity preservation for $\tau < 1/2$, statement (vi) follows. □

4. Conclusions

Theoretical foundations for PDE-based shock filtering has long been considered to be a hopelessly difficult problem. In this paper we have shown that it is possible to obtain both an analytical solution and well-posedness by considering the space-discrete case where the partial differential equation becomes a dynamical system of ordinary differential equations (ODEs). Moreover, corresponding results can also be established in the fully discrete case when an explicit time discretisation is applied to this ODE system.

We are convinced that this basic idea to establish well-posedness results for difficult PDEs in image analysis by considering the semidiscrete case is also useful in a number of other important PDEs. While this has already been demonstrated for nonlinear diffusion filtering [13, 10], we plan to investigate a number of other PDEs in this manner, both in the one- and the higher-dimensional case. This should give important theoretical insights into the dynamics of these experimentally well-performing nonlinear processes.

References

[1] L. Alvarez and L. Mazorra. Signal and image restoration using shock filters and anisotropic diffusion. *SIAM Journal on Numerical Analysis*, 31:590–605, 1994.

[2] R. W. Brockett and P. Maragos. Evolution equations for continuous-scale morphology. In *Proc. IEEE International Conference on Acoustics, Speech and Signal Processing*, volume 3, pages 125–128, San Francisco, CA, March 1992.

[3] G. Gilboa, N. A. Sochen, and Y. Y. Zeevi. Regularized shock filters and complex diffusion. In A. Heyden, G. Sparr, M. Nielsen, and P. Johansen, editors, *Computer Vision – ECCV 2002*, volume 2350 of *Lecture Notes in Computer Science*, pages 399–413. Springer, Berlin, 2002.

[4] F. Guichard and J.-M. Morel. A note on two classical shock filters and their asymptotics. In M. Kerckhove, editor, *Scale-Space and Morphology in Computer Vision*, volume 2106 of *Lecture Notes in Computer Science*, pages 75–84. Springer, Berlin, 2001.

[5] P. Kornprobst, R. Deriche, and G. Aubert. Nonlinear operators in image restoration. In *Proc. 1997 IEEE Computer Society Conference on Computer Vision and Pattern Recognition*, pages 325–330, San Juan, Puerto Rico, June 1997. IEEE Computer Society Press.

[6] H. P. Kramer and J. B. Bruckner. Iterations of a non-linear transformation for enhancement of digital images. *Pattern Recognition*, 7:53–58, 1975.

[7] S. Osher and L. Rudin. Shocks and other nonlinear filtering applied to image processing. In A. G. Tescher, editor, *Applications of Digital Image Processing XIV*, volume 1567 of *Proceedings of SPIE*, pages 414–431. SPIE Press, Bellingham, 1991.

[8] S. Osher and L. I. Rudin. Feature-oriented image enhancement using shock filters. *SIAM Journal on Numerical Analysis*, 27:919–940, 1990.

[9] S. Osher and J. A. Sethian. Fronts propagating with curvature-dependent speed: Algorithms based on Hamilton–Jacobi formulations. *Journal of Computational Physics*, 79:12–49, 1988.

[10] I. Pollak, A. S. Willsky, and H. Krim. Image segmentation and edge enhancement with stabilized inverse diffusion equations. *IEEE Transactions on Image Processing*, 9(2):256–266, February 2000.

[11] L. Remaki and M. Cheriet. Numerical schemes of shock filter models for image enhancement and restoration. *Journal of Mathematical Imaging and Vision*, 18(2):153–160, March 2003.

[12] J. G. M. Schavemaker, M. J. T. Reinders, J. J. Gerbrands, and E. Backer. Image sharpening by morphological filtering. *Pattern Recognition*, 33:997–1012, 2000.

[13] J. Weickert. *Anisotropic Diffusion in Image Processing*. Teubner, Stuttgart, 1998.

[14] J. Weickert. Coherence-enhancing shock filters. In B. Michaelis and G. Krell, editors, *Pattern Recognition*, volume 2781 of *Lecture Notes in Computer Science*, pages 1–8, Berlin, 2003. Springer.

[15] M. Welk, J. Weickert, I. Galić. Theoretical Foundations for 1-D Shock Filtering. Preprint, Saarland University, Saarbruecken, 2005.